




Article

Theoretical Study on Freezing Separation Pressure of Clay Particles with Surface Charge Action

Xiaoyan Liu ¹, Hua Cheng ^{1,2,*}, Hanqing Chen ¹, Longhui Guo ¹, Yu Fang ¹ and Xuesong Wang ¹

¹ School of Civil Engineering and Architecture, Anhui University of Science and Technology, Huainan 232001, China

² School of Resources and Environmental Engineering, Anhui University, Hefei 230601, China

* Correspondence: hcheng@aust.edu.cn

Abstract: This study aimed to clarify the mechanism of the effect of surface charge of clay particles on the separation pressure between adjacent frozen clay particles. A general mathematical model of separation pressure between adjacent spherical clay particles was given based on the extended colloidal stability (DLVO) theory; it was introduced into the frost heave process, and the functional expression of separation pressure and freezing temperature between clay particles was derived by using the relationship between the pore throat's radius and freezing temperature, which was verified by the existing experimental results. Finally, the effects of the freezing temperature, mineral species and solution concentration on the freezing separation pressure and ice-lens growth were analyzed. Our results show that the surface distance of adjacent charged bodies is a single-valued function of their separation pressure, but the freezing temperature is the main factor affecting the separation pressure between adjacent frozen clay particles; the separation pressure between adjacent clay particles is proportional to its surface-charge density. For the same particle spacing, the separation pressures of kaolinite and illite are not much different, but they are both about one order of magnitude lower than montmorillonite; the separation pressure between clay particles is negatively correlated with the solution concentration. When the solution concentration is less than $0.1 \text{ mol}\cdot\text{m}^{-3}$, the effect of the solution concentration on the separation pressure between particles is negligible. The research results can provide a theoretical reference for improving the existing geotechnical frost heave theory.

Keywords: clay particles; DLVO theory; electrical properties; separation pressure; freezing temperature; ice lens



Citation: Liu, X.; Cheng, H.; Chen, H.; Guo, L.; Fang, Y.; Wang, X. Theoretical Study on Freezing Separation Pressure of Clay Particles with Surface Charge Action. *Crystals* **2022**, *12*, 1304. <https://doi.org/10.3390/cryst12091304>

Academic Editor: Zhaohui Li

Received: 26 August 2022

Accepted: 12 September 2022

Published: 15 September 2022

Publisher's Note: MDPI stays neutral with regard to jurisdictional claims in published maps and institutional affiliations.



Copyright: © 2022 by the authors. Licensee MDPI, Basel, Switzerland. This article is an open access article distributed under the terms and conditions of the Creative Commons Attribution (CC BY) license (<https://creativecommons.org/licenses/by/4.0/>).

1. Introduction

In the negative temperature environment, the formation of frozen ice and the occurrence of water migration in the soil make the soil frost heave [1]. The occurrence of frost heave usually leads to the destruction of buildings (structures), as well as infrastructure such as roads [2] and underground pipelines [3], which seriously threatens their operational safety. The distribution area of permafrost and seasonally frozen soil in my country accounts for 21.5% and 53.5% of the national area, respectively, making it the third largest country in the world in terms of permafrost area distribution. Therefore, the research on the mechanism of frost heave is the main problem in the design and construction of the whole cold region.

Frost heaving can be divided into in situ frost heaving and segregation frost heaving, of which segregation frost heave occupies the dominant position [4]. At present, when domestic and foreign scholars [5–7] study the one-dimensional frost heave system, the soil during the freezing process is roughly divided into three regions: the frozen area, the frozen fringe and the unfrozen area (as shown in Figure 1). Among them, the freezing fringe refers to the region between the warmer end of the ice lens and the freezing front [8], but the freezing fringe does not exist forever [9], and its proposal has a milestone significance for

the study of the frost-heaving mechanism. Xia [10] conducted a one-dimensional freezing test on Devon silt through digital photography technology and found that there were cracks at the frozen fringe, and the cracks appeared before the horizontal lens and vertical ice vein. Lukas et al. [11], Konard and Duquennoi [12] also found that the formation of the new lens was related to the cracking of the soil at the frozen fringe through experimental observation. Based on this, Amatch et al. [13] proposed to take the crack initiation point on the soil freezing characteristic curve (SFCC) as the ice-crystal invasion point (IEV) as the criterion for the formation of new lens and verified the rationality of the hypothesis through experiments. Zhou et al. [14] proposed that once the initial conditions of new lenses at the freezing fringe are determined, the growth of a single ice lens can be extended to the entire frost heave model. Therefore, clarifying the intrinsic relationship between soil cracks and the formation of new lenses is the first step in studying the mechanism of frost heave due to segregation.

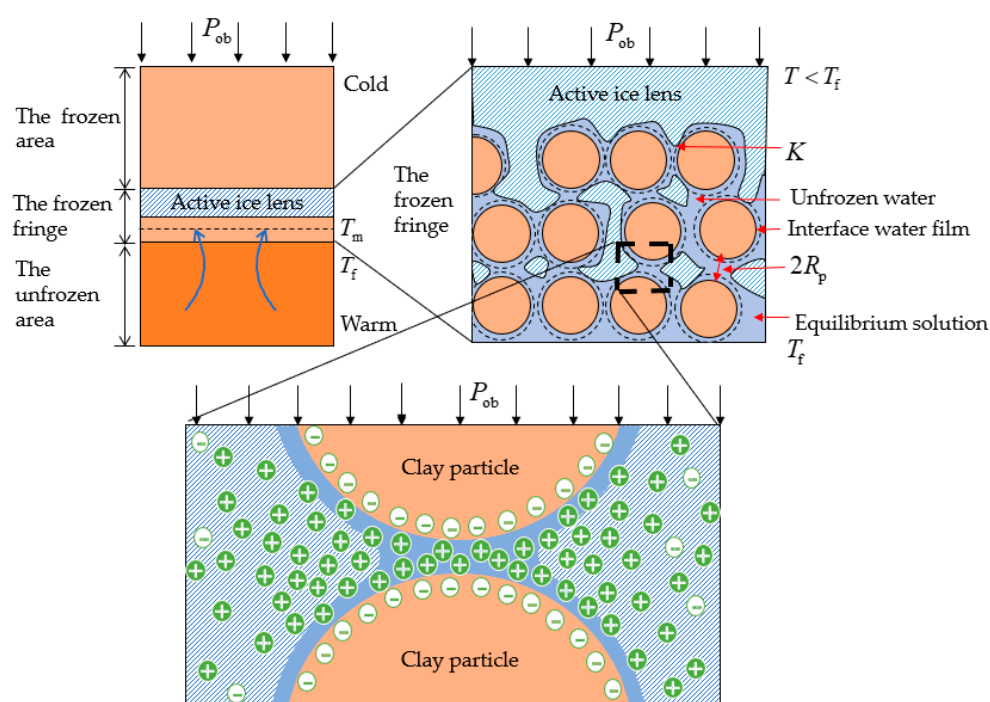


Figure 1. Theoretical model of freezing separation pressure, considering the effect of surface charge on clay particles.

In the freezing process, the cracks of the soil are formed before the pore ice reaches the maximum [15], which is mainly limited by the cohesion of the soil and the geometric undercooling [16]. Miller et al. [17] used the Clapeyron equation to estimate ice pressure based on the Harlan model [18] and found that, under certain conditions, the effective compressive stress between soil particles is zero, which, in principle, can separate the clay particles. This concept of soil separation pressure was first put forward by Gilpin, but its concept is not clear and difficult to determine [19,20]. In subsequent studies, many scholars [21] used the sum of the external pressure and the critical tensile strength of the soil as the soil separation strength, ignoring the influence of the special electrical properties of the clay particle surface on the soil separation pressure during the freezing process; it is difficult to fully reveal the intrinsic connection between cracks and the formation of new lens bodies. Therefore, it is of positive significance to improve and explore the theory of frost heave to carry out research on the action mechanism of clay-surface electrical properties on the separation pressure between clay particles.

The purpose of this study was to establish a theoretical model of separation pressure between frozen clay particles, considering the interaction of clay surface forces, to reveal the intrinsic relationship between soil cracks and the formation of new lenses and to pro-

vide theoretical references for improving the research on frost heave mechanism. This study starts from the special electrical properties of the clay particles. Firstly, the general expression of the mathematical model of the separation pressure between adjacent clay particles was established based on the extended DLVO theory. Secondly, the relationship between the pore throat's radius and intergranular separation pressure during ice separation was taken as the connection point, and then the characterization relationship between intergranular separation pressure and freezing temperature was established; then the ice pressure was used as the destructive force of the contact between frozen clay particles, and the generalized expression of the separation pressure between frozen clay particles was obtained through the meso-mechanical equilibrium relationship of soil. The effects of freezing temperature, mineral species and solute concentration on freezing separation pressure and ice-lens growth were analyzed. The research results provide a theoretical reference for the in-depth understanding of the frost heave characteristics and mechanism of soil.

2. Theoretical Model of Freezing Separation Pressure, Considering Surface Charge of Clay Particles

2.1. Theoretical Model of Freezing Separation Pressure

Due to the surface force interaction caused by the charge overlap at the interface of charged particles, the water film pressure between two charged particles is different from the pressure at the same depth in the reservoir containing these particles. This difference in pressure is referred to as the separation pressure [22]. Among them, the surface forces involved mainly include the Van der Waals forces, P_h^m ; the electrostatic forces, P_h^e ; and the structural forces, P_h^s . Among them, P_h^e and P_h^s are considered to be positive for clay/clay systems, and P_h^m is positive forces. Corresponding to the suction and pressure in the mechanical sense, respectively, the equilibrium relationship between the two forces determines the symbol of the separation pressure [23]. When the net separation pressure is negative, it means that the gravitational component dominates in a small distance, and when it is positive, it means that the repulsive component dominates. However, for large-aperture charged media, because there is no charge overlap between the adjacent interfaces, the water-film-pressure variable is the same as that in the equilibrium solution, so this separation pressure is effective only in the presence of microcracks [24].

For the one-dimensional freezing system, the soil skeleton is compressed in the process of ice segregation. When the pressure inside the pore reaches the local maximum at the pore diameter, the unfrozen water film on the clay surface is no longer thinned with the occurrence of freezing, and the slow flow velocity can be regarded as a quasi-steady state [10]. In order to meet the further occurrence of freezing, the thermal molecular force between the ice–soil interface pushes the clay particles to the warmer end to provide space for further growth of ice crystals [25]; at this time, tiny cracks are formed between adjacent clay particles [26]. When the curvature of the ice crystal is $K > 2/R_p$, the ice crystal can further grow to the crack, forming a new ice lens [27]. It was therefore concluded that the separation pressure, P_h , between adjacent clay particles during freezing was closely related to the critical pore throat's radius, R_p , and ultimately affects the formation of new ice lenses. Therefore, when considering the surface electrical properties of clay particles, the separation pressure between frozen clay particles can be equivalent to the ice pressure that can resist the interaction of surface forces and external loads.

To clarify the influence mechanism of the surface electrical properties of clay particles on the separation pressure between frozen clay particles, in this study, a group of adjacent clay particles surrounded by ice was selected as the object of study. It was assumed that there was an external pressure acting on the cross-section of the particles, ignoring the influence of the surrounding clay particles, as shown in Figure 1.

2.2. Basic Assumption

In this study, the following assumptions were made to control the model equation:

1. Clay particles are uniform and incompressible spheres;
2. The surface charge of the clay particles is uniformly distributed, and the ion-diffusion law obeys the Boltzmann distribution;
3. The positive and negative ions in the solution have the same number of charges, and the whole system is electrically neutral.

3. Separation Pressure between Clay Particles

3.1. Separation Pressure between Parallel Plates

Based on the colloidal stability (DLVO) theory, the electrical properties of the adjacent charged surfaces in the equilibrium solution can form a parallel-plate capacitor with a distance, h , and the total separation pressure generated by the interaction of the surface force between the charged parallel clay platelets can be expressed as follows [28]:

$$P_h^{tot} = P_h^m + P_h^e + P_h^s \quad (1)$$

where P_h^{tot} is the total separation pressure of the charged parallel clay platelets, Pa.

Although the strength of Van der Waals force, P_h^m , is not as strong as the Coulomb force or hydrogen-bond interaction force, it is widespread and plays a major role when the spacing is both small and large. The Van der Waals force per unit area can be expressed as follows:

$$P_h^m = -\frac{A_H}{6\pi h^3} \quad (2)$$

Corresponding to the weak gravitational force between adjacent clay surfaces, it plays a central role in the intermolecular attractive force. The value h is the distance between parallel platelets. A_H is the Hamaker constant that depends on the mineralogical nature of the surface; usually, the value range of it is $10^{-19} \sim 10^{-20}$ J. For clay in aqueous solution, 5×10^{-20} J [29] was used as the Hamaker constant.

The electrostatic component of the separation pressure can be accounted for by using the following relationship:

$$P_h^e = \frac{k^2}{2\pi} Z e^{-kh} \quad (3)$$

where Z is the interaction constant that just depends on the mineralogical nature of the surface, $\text{J}\cdot\text{m}^{-1}$. It can be expressed as follows:

$$Z = 64\pi\epsilon\epsilon_0 \left(\frac{k_B T}{e}\right)^2 \tan h^2 \left(\frac{ze\varphi_0}{4k_B T}\right) \quad (4)$$

where k^{-1} is the Debye length, which provides the diffuse layer thickness, m^{-1} . It depends on the properties of the equilibrium solution and is independent of the surface properties of the charged object (such as charge and potential). It can be expressed as follows:

$$k = \left(\frac{2N_A c_0 z^2 e^2}{\epsilon\epsilon_0 k_B T}\right)^{\frac{1}{2}} \quad (5)$$

where N_A is the Avogadro constant ($N_A \approx 6.022 \times 10^{23} \text{ mol}^{-1}$); c_0 is the concentration of the equilibrium solution, $\text{mol}\cdot\text{m}^{-3}$; e is the elementary electric charge ($e \approx 1.602 \times 10^{-19} \text{ C}$); z is the absolute value of ionization valence in symmetrical electrolyte solution, $z = 1$ for NaCl; ϵ is the relative permittivity of the electrolyte solution ($\epsilon \approx 78.4$); ϵ_0 is the permittivity of a vacuum ($\epsilon_0 \approx 8.854 \times 10^{-12} \text{ F}\cdot\text{m}^{-1}$); and k_B is the Boltzmann constant ($k_B \approx 1.38 \times 10^{-23} \text{ J}\cdot\text{K}^{-1}$).

When the distance between charged parallel plates is very small (1.5~5 nm), the structural component of the separation pressure needs to be introduced. Compared with

the Van der Waals force and electrostatic force, the theory of structural force has not been fully developed, and the exponential relation can be expressed as follows [30]:

$$P_d^s = k_0 \exp\left(-\frac{h}{\lambda}\right) \quad (6)$$

where k_0 is the structural force coefficient ($k_0 \approx 1.5 \times 10^{10}$ Pa), and λ characterizes the range of structural forces' action ($\lambda \approx 0.05$ nm).

Therefore, we have the following:

$$P_h^{tot} = -\frac{A_H}{6\pi h^3} + 32k\epsilon\epsilon_0 \left(\frac{k_B T}{e}\right)^2 \tanh^2\left(\frac{ze\varphi_0}{4k_B T}\right) \exp(-kh) + k_0 \exp\left(-\frac{h}{\lambda}\right) \quad (7)$$

For smaller electrical potential, $\tanh(ze\varphi_0/4k_B T)$ is approximate to the function itself, and we can obtain the following:

$$\tanh\left(\frac{ze\varphi_0}{4k_B T}\right) \approx \frac{ze\varphi_0}{4k_B T} \quad (8)$$

Equation (7) can be simplified as follows:

$$P_h^{tot} = -\frac{A_H}{6\pi h^3} + 2z^2\varphi_0^2 k^2 \epsilon\epsilon_0 \exp(-kh) + k_0 \exp\left(-\frac{h}{\lambda}\right) \quad (9)$$

3.2. Separation Pressure between Spherical Clay Particles

Under the same applied force, the relationship between the two surfaces and the two planes is obviously different [31]; therefore, when the particle radius is much larger than the particle spacing, in order to improve the accuracy of calculation, it is necessary to transform the above parallel plate model to obtain the separation-pressure calculation formula between adjacent spherical particles.

In order to solve the separation pressure between adjacent clay particles, it is necessary to determine the effective contact area between the adjacent clay particles in the ideal model.

The geometric relationship of clay particles with a distance of is shown in Figure 2, where R_1 and R_2 represent the radius of adjacent clay particles, respectively. The hypothesis is $R_1 = R_2 = R \gg h$, where R is the radius of a uniform spherical clay particle. Using the Pythagorean theorem, the geometric relationship between adjacent clay particles can be expressed as follows:

$$\begin{cases} r_1^2 = r_2^2 \approx 2Rx_1 \\ x = h + x_1 + x_2 = h + \frac{r_1^2}{R} \\ A_{ss} = \pi r_1^2 = \pi r_2^2 \end{cases} \quad (10)$$

where x_1 and x_2 are the measurable ranges of force (usually the same dimension as particle size), and A_{ss} is the effective contact area between adjacent clay particles:

$$\begin{cases} dx = \frac{2r_1}{R} dr_1 \\ dA_{ss} = 2\pi r_1 dr_1 \approx \pi R dx \end{cases} \quad (11)$$

According to Derjaguin et al. [32], the transformation relationship between the surface force of the distance between objects of any shape and the surface force $f(x)$ per unit area between two flat plates is proposed as follows:

$$P(x) = \int_h^\infty f(x) \frac{dA_{ss}}{dx} dx \quad (12)$$

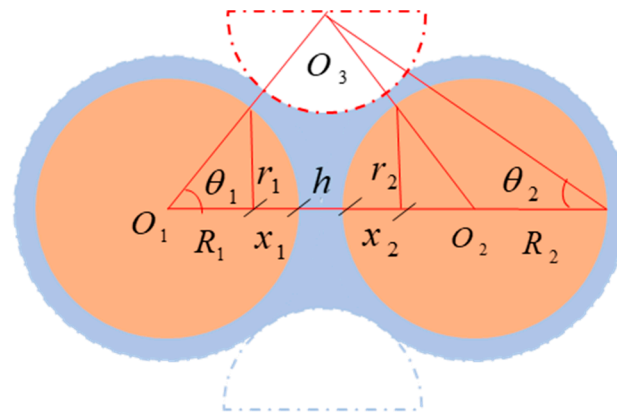


Figure 2. Geometric relationship of spherical clay particles with spacing.

By substituting Equations (10) and (11) into (12), the actual separation pressure acting between two equal-radius clay particles can be obtained as follows:

$$\begin{aligned} P(h) &= \pi R \int_h^\infty P^{tot}(x) dx \\ &= -\frac{A_H R}{12h^2} + 2z^2 \varphi_0^2 R k \pi \epsilon \epsilon_0 \exp(-kh) + \pi R \lambda k_0 \exp\left(-\frac{h}{\lambda}\right) \end{aligned} \quad (13)$$

Therefore, the forces and energies of all surface interactions can be derived from the local radius of the surface through a scaling factor, which has been experimentally verified [30].

Furthermore, the surface electrical potential, φ_0 , can be represented by the surface-charge density, ρ_e [31]:

$$\rho_e = \epsilon \epsilon_0 k \varphi_0 \quad (14)$$

Therefore, Equation (13) can be sorted out, and the separation pressure caused by the interface action of adjacent clay particles with a distance of can be expressed as follows:

$$P(h) = R \left[-\frac{A_H}{12h^2} + 2\pi \rho_e^2 z^2 \exp(-kh) + \pi \lambda k_0 \exp\left(-\frac{h}{\lambda}\right) \right] \quad (15)$$

Obviously, in a given electrolyte solution, the separation pressure between adjacent clay particle interfaces is a single value function of the water film thickness between particles and is proportional to the particle radius.

Cheng et al. [33] obtained the initial pore size distribution of saturated silty clay through low-field NMR test, of which about 96.91% is less than 0.3 μm in pore size. When the particle spacing is 0.3 μm , the surface force to be overcome for separating clay particles per unit area is -9.83×10^{-2} Pa; when the particle spacing is 0.03 μm , the surface force to be overcome for separating clay particles per unit area is -98.3 Pa; when the particle spacing is 0.003 μm , the surface force to be overcome for separating clay particles per unit area is -9.83×10^4 Pa. Therefore, the separation pressure between particles gradually decreases with the increase of the distance.

4. Separation Pressure between Adjacent Frozen Clay Particles during Segregation

4.1. Meso-Mechanical Equilibrium Equation between Frozen Clay Particles

During the separation, with the continuous growth of ice crystals, the interaction between the surface force of ice and clay gradually increases, which reduces the ice point of the convex surface of ice crystals near the adjacent clay particles, so the ice crystals will not be filled to the wedge-shaped apex [34]. According to the principle of continuum mechanics, pore water always exists at the apex of wedge, forming undisturbed pore water pressure, p_l . With the occurrence of freezing, when the ice pressure reaches the local

maximum, as shown in Figure 3, the mechanical equilibrium relationship between the ice crystal and the pore wall surface satisfies the following equation:

$$p_s - p_l = \sigma_{sl}K \quad (16)$$

where p_s is ice pressure, Pa; p_l is water pressure, Pa; σ_{sl} is the ice-water interfacial tension ($\sigma_{sl} \approx 29 \times 10^{-3} \text{ J}\cdot\text{m}^{-2}$); and K is the curvature of the ice-water interface, m^{-1} .

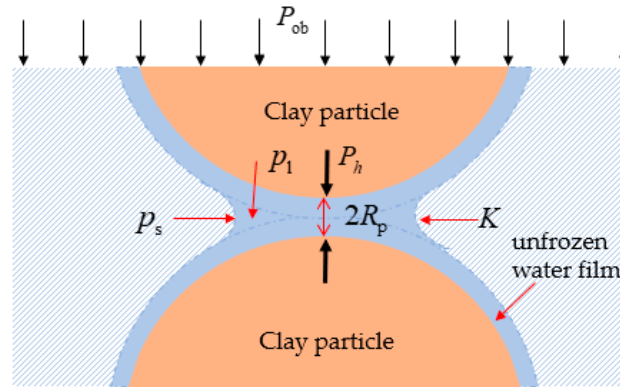


Figure 3. Micromechanical equilibrium relationship between adjacent clay particles during segregation.

The density difference between ice and water was neglected. It can be known from the Clapeyron equation that, when the local phase equilibrium is satisfied at the interface, the relationship between ice pressure, p_s , and pore water pressure, p_l , can be expressed as follows:

$$p_s - p_l = \rho q_m \frac{T_m - T}{T_m} \quad (17)$$

where ρ is density ($\rho \approx 917 \text{ kg}\cdot\text{m}^{-3}$); q_m is latent heat of phase transition per unit mass ($q_m \approx 3.35 \times 10^5 \text{ J}\cdot\text{kg}^{-1}$); T is freezing temperature, K; and T_m is the melting temperature ($T_m \approx 273.15 \text{ K}$).

By combining (16) and (17), we can obtain the following wedge-shaped area curvature expression:

$$K = \frac{\rho q_m}{\sigma_{sl}} \frac{T_m - T}{T_m} \quad (18)$$

Since the separation pressure, P_h , between adjacent clay particles during the freezing process is closely related to the size of the pore throat's radius, R_p , in the critical state, when the equilibrium curvature, K , of the separated ice is greater than the pore throat's radius, $2/R_p$, the ice crystal can further grow and form a new ice lens. Therefore, the functional relationship between the pore throat's radius and the freezing temperature can be expressed as follows:

$$R_p = \frac{2}{K} = \frac{2\sigma_{sl}}{\rho q_m} \frac{T_m}{T_m - T} \quad (19)$$

where R_p is the characteristic radius of the pore's throat, m.

From the simultaneous Equations (18) and (19), the temperature at which the ice crystals enter the pores at the critical point for further growth of ice crystals can be obtained as follows:

$$T_{ice} = T_m - \frac{2T_m\sigma_{sl}}{\rho_s q_m R_p} \quad (20)$$

Moreover, the above equation is consistent with the temperature expression of ice crystal entering the pore at this critical point obtained by Pepper et al. [35] according to the Gibbs Thomson equation.

Therefore, two conditions of the growth of the segregated ice can be obtained: firstly, when $T_m \geq T \geq T_{ice}$, the ice lenses grow before entering pores of clay particles. In this case, the ice lens does not fill the whole pore, the water migrates to the frozen fringe easily,

and the ice lens grows rapidly; secondly, when $T < T_{ice}$, the ice lens enters the clay pores forming a frozen fringe [27]. In this case, the growth rate of the ice lens is slow because the entry of the ice lens into the clay pore hinders the migration of water to the growing lens. Thus, the purpose of this study was to investigate the separation pressure between adjacent clay particles during the freezing process; only the situation before ice crystals enter the clay cracks was considered.

Since the aqueous solution in the saturated clay is a continuous medium, it can be considered that the thickness of the stable water film between adjacent clay particles is equal to two times that of the pore throat's radius. As shown in Figure 3, the relationship between the pore throat's radius, R_p , and the distance, h , of adjacent clay particles can be expressed as follows:

$$h = 2R_p \quad (21)$$

By substituting Equation (21) into (15), the characteristic relationship between the pore throat's radius, R_p , and the separation pressure, P_h , is obtained as follows:

$$P(R_p) = -\frac{A_H R}{48R_p^2} + 2\pi R \rho_c^2 z^2 \exp(-2R_p k) + \pi R \lambda k_0 \exp\left(-\frac{2R_p}{\lambda}\right) \quad (22)$$

Equation (19) shows that R_p decreases with the increase of freezing temperature, T . In order to reduce unknown parameters, the temperature function of separation pressure between adjacent clay particles prepared by Equations (19), (21) and (22) is as follows:

$$P(T) = -\frac{A_H R}{12\left(\frac{4\sigma_{sl}}{\rho q_m} \frac{T_m}{T_m - T}\right)^2} + 2\pi R \rho_c^2 z^2 \exp\left(-k \frac{4\sigma_{sl}}{\rho q_m} \frac{T_m}{T_m - T}\right) + \pi R \lambda k_0 \exp\left(-\frac{4\sigma_{sl}}{\lambda \rho q_m} \frac{T_m}{T_m - T}\right) \quad (23)$$

4.2. Separation Pressure between Frozen Clay Particles

The concept of separation pressure between soil particles during freezing was first put forward by Gilpin [36], and it is considered that the separation pressure is the critical pressure causing soil failure, similar to the "internal" pressure measured by Williams and Wood [37]. The French Geotechnical Laboratory [38] obtained the total stress range of the frozen soil from 20 to 80 kPa by testing the frozen soil stress in the free state; Mackay [39] proved that the total stress of typical seasonal frozen soil ranges from 50 to 150 kPa. When considering the surface electrical properties of clay particles, the separation pressure between frozen clay particles can be defined as follows: in the one-dimensional freezing process, when the unfrozen water film on the clay surface is no longer thinned with the freezing, we can obtain the sum of the separation pressure between particles and the ice pressure triggered by the interaction of the surface forces of adjacent clay particles. In this case, the meso-mechanical equilibrium between particles can be expressed as follows:

$$p_s + P(R_p) = P_{ob} + \sigma_{sl} K_0 \quad (24)$$

where K_0 is the curvature of spherical clay particles; $K_0 = 2/R$. At the beginning of freezing, the external pressure is mainly borne by the clay skeleton. With the growth of the ice lens, the ice pressure in the freezing fringe can reach the local maximum value. When the clay particles are separated, they replace the clay skeleton to bear the external pressure to form a new ice lens. When the ice pressure, p_s , is used as the destructive force to separate the frozen clay particles, let the following be:

$$p_s = P_{sep} \quad (25)$$

where P_{sep} is the frozen-clay-particle separation pressure, Pa. By substituting Equation (25) into (24), we can obtain the following:

$$P_{sep} = P_{ob} + \frac{2}{R}\sigma_{sl} - P(R_P) \quad (26)$$

In order to reduce the calculation parameters, Equations (20) and (22) are substituted into (26) to obtain the separation-pressure expression of the adjacent frozen clay particles:

$$\begin{aligned} P_{sep} &= P_{ob} + \frac{2}{R}\sigma_{sl} - P(T_{ice}) \\ &= P_{ob} + \frac{2}{R}\sigma_{sl} - \pi R \left[\frac{\frac{A_H}{12\pi\left(\frac{4\sigma_{sl}}{\rho q_m} \frac{T_m}{T_m - T_{ice}}\right)^2} - 2\rho_e^2 z^2 \exp\left(-\frac{4k\sigma_{sl}}{\rho q_m} \frac{T_m}{T_m - T_{ice}}\right)}{-\lambda k_0 \exp\left(-\frac{4k\sigma_{sl}}{\lambda \rho q_m} \frac{T_m}{T_m - T_{ice}}\right)} \right] \end{aligned} \quad (27)$$

4.3. Validation Analysis

According to the review of Gilpin's [36] separation-pressure theory, Gilpin proposed that the separation pressure in the freezing process refers to the critical pressure causing soil damage. The particle shape (such as particle radius and interface curvature) and interface curvature (such as external pressure and temperature) were considered. Gilpin obtained the following expression of separation pressure between adjacent frozen clay particles:

$$P_{Gsep} = P_{ob} + \frac{2\sigma_{sl}}{R} f(P_R) \quad (28)$$

where σ_{sl} is the solid-liquid interfacial tension, $\text{N}\cdot\text{m}^{-1}$; and P_R is the geometric characteristic parameter of unfrozen water film, which can be expressed as follows:

$$P_R = \frac{\rho_l q_m R \Delta T}{2\sigma_{sl} T_m} \quad (29)$$

where ρ_l is the density of water, ($\rho_l \approx 1000 \text{ kg}\cdot\text{m}^{-3}$). The approximate value of $f(P_R)$ can be expressed as follows:

$$f(P_R) = \frac{P_R}{7.5} \left[1 - \exp\left(-\frac{7.5}{P_R}\right) \right] \quad (30)$$

Azmatch et al. [13], based on the similarity between the soil-water freezing characteristic curve and the soil-water curve, it was proposed that the initial value of the lens is close to the ice entering pore value, and then through the one-dimensional freezing test of the open system, it was obtained that the pressure to be overcome when the ice enters the pore of Devon silty clay under the external pressure of 100 kPa, 200 kPa and 400 kPa is 175 kPa, 250 kPa and 450 kPa, respectively. The temperatures of ice entering the pores are -0.16°C , -0.19°C and -0.40°C , respectively. In this paper, the surface-charge density of clay is $0.133 \text{ C}\cdot\text{m}^{-2}$, and the particle size of clay is $7.7 \times 10^{-7} \text{ m}$. The main calculation parameters were substituted into the theoretical calculation model of the Gilpin interparticle separation pressure and the theoretical calculation model of this study, and the relevant calculation results are shown in Table 1. The theoretical value obtained in this study is in good agreement with the Azmatch's test value, but there is a certain error with the Gilpin theoretical value. The reason is mainly composed of two parts. Firstly, this study assumes that the clay particles are uniform spheres and ignores the geometric characteristics of the clay particles when considering the contribution of the surface tension at the pore's throat to the separation pressure between the clay particles. Therefore, when the characteristic parameters of the clay-surface geometry are added to this research model, it can show a good agreement with the predicted value of Gilpin theory. Second, the influence of surface force on the separation pressure between particles is smaller than the external pressure and the surface tension of the solid-liquid interface, it is usually ignored

in the study of separation pressure between particles. In this study, based on the surface electrical properties of clay particles, the contribution of the interaction of surface forces between adjacent clay particles to the separation pressure between clay particles was taken into account. Therefore, it can be considered that the theoretical model of this study is reasonable and feasible.

Table 1. Comparative analysis table of experimental values and theoretical calculation results.

Temperature (°C)	VE1 (MPa)	VE2 (MPa)	VE3 (MPa)	EC1 (%)	EC2 (%)	EC3 (%)
−0.16	0.175	0.175	0.122	0.2	30	43
−0.19	0.250	0.275	0.222	10	11.2	23.8
−0.40	0.450	0.475	0.422	5.5	6.2	12.6

Annotation: VE1 = Azmatch's test value, VE2 = the theoretical value of this study, VE3 = value calculated by Gilpin theory; EC1 = the percentage error between the theoretical value in this study and the Azmatch test value, EC2 = percentage error between the theoretical value of Gilpin and the experimental value of Azmatch, EC3 = the percentage of error between the theoretical value of this study and Gilpin's theoretical value.

When the value of P_R is larger, $f(P_R) \approx 1$. Therefore, we obtain the following:

$$P_{Gsep} = P_{ob} + \frac{2\sigma_{sl}}{R} \quad (31)$$

The simultaneous Formulas (27) and (31) can obtain the following:

$$P_{Gsep} - P_{sep} = P(T_{ice}) \quad (32)$$

From Equation (32), it can be considered that, when R is large, the error between the separation pressure between clay particles proposed by Gilpin, P_{Gsep} , and the theoretical formula of frozen clay separation pressure obtained in this study, P_{sep} , is the separation pressure caused by the interaction of surface forces. The author discusses the error in detail in Section 5. Because the separation pressure between clay particles caused by surface force only acts on microcracks, when the distance between adjacent clay particles exceeds a certain threshold, $P_{Gsep} \approx P_{sep}$, the theoretical model proposed in this study is in good agreement with the proposed model by Gilpin. Therefore, this study can be regarded as a generalized form of the theoretical formula of separation pressure between adjacent frozen clay particles proposed by Gilpin.

5. Discussion

In recent years, the global surface temperature has increased due to climate warming, and the removal of surface vegetation or buildings will also affect surface temperature, thereby accelerating the degradation of permafrost [40]. These surface changes have had a severe negative impact on the thermal stability of transportation infrastructure in high-altitude and high-latitude permafrost regions [41]. Therefore, analyzing the influencing factors of the separation pressure between frozen clay particles has a positive effect on the further study of frost heave mechanism. In the actual engineering environment, there are many factors that affect the separation pressure between frozen clay particles, such as freezing temperature, mineral types, solute concentration and so on. Due to the difference in mineral composition and formation conditions, each fine-grained soil will form a different average density and particle orientation. The common mineral components in clay are montmorillonite, illite and kaolinite. Through experimental analysis, Gee et al. [42] showed that the charge density, ρ_e , of the clay surface can be estimated by the cation exchange capacity (CEC) and specific surface area (S) of clay minerals, namely $\rho_e = -\text{CEC}/S$. Table 2 shows the basic parameters and basic calculated value distribution obtained according to the existing literature [43]. Since the thermodynamic temperature has no significant influ-

ence on the electric potential of the double layer, the values of $1/k$ and φ_0 that are calculated according to the data in the Table 2 are also applicable to the range of 0~25 °C [44].

Table 2. Clay mineral composition and main calculation parameters.

Clay Mineral	CEC (mequiv·(100) ⁻¹)	S (m ² ·g ⁻¹)	ρ_e (C·m ⁻²)	1/k (nm)	φ_0 (V)
Kaokinite	5	15	0.322	3.02	3.16×10^{-3}
Illite	25	84	0.287	3.02	2.84×10^{-3}
Montmorillonite	100	800	0.121	3.02	1.25×10^{-3}

Annotation: T = 293 K. NaCl: $c_0 = 10 \text{ mol}\cdot\text{m}^{-3}$.

Since the proportional enlargement or reduction of the function dependent variable in the calculation process does not affect the discussion of its change trend [45,46], for a more intuitive expression, this paper used the same proportional reduction of the separation pressure between clay particles to obtain P_h/R in the following discussion. This indicates the effect of different factors on the separation pressure between frozen clay particles.

5.1. Effect of Freezing Temperature on Separation Pressure between Adjacent Clay Particles

Substitute the relevant parameters in Table 2 into Equation (23) to obtain the variation curve of separation pressure between frozen clay particles with temperature, as shown in Figure 4. With the increase of freezing temperature, the separation pressure between frozen clay particles shows gravitational action and increases exponentially, which is in good agreement with the research results of Watanabe et al. [47]. This is because, in the one-dimensional freezing process, with the continuous development of the freezing process, the thermal molecular force between the ice and the clay wall pushes the clay particles to the warmer end, causing the adjacent clay wall to form microcracks, and the clay particles are rapidly surrounded by the liquid. The diffusion layers from the surface of each clay particle will overlap and generate a repulsive force. These repulsive forces can effectively reduce the cohesion between adjacent clay particles, thereby reducing the normal component between contact particles and promoting the development of soil cracks [44]. Finally, the surface forces between adjacent clay particles appear as weak gravity and increase with the decreases of freezing temperature.

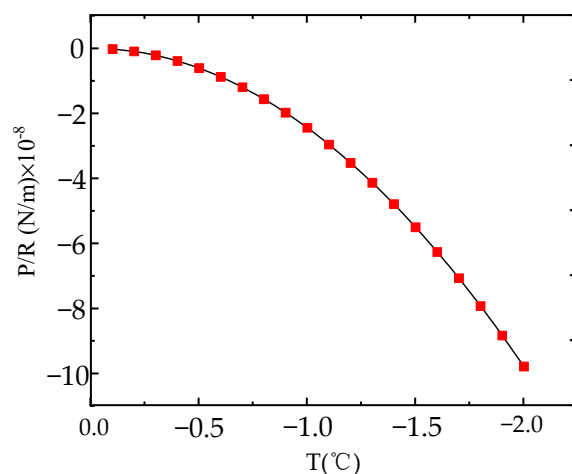


Figure 4. Effect of temperature on separation pressure between frozen clay particles.

5.2. Effect of Mineral Types on Separation Pressure between Adjacent Particles

Figure 5 shows that the different mineral types of clay vary with the distance between particles when the freezing temperature is $-0.68 \text{ }^\circ\text{C}$. When the particle spacing is equal

to 2 nm, the separation pressures between kaolinite, illite and montmorillonite are 0.335R, 0.266R and 0.047R, respectively; When the particle spacing is equal to 4 nm, the separation pressures between kaolinite, illite and montmorillonite are 0.173R, 0.137R and 0.024R, respectively; and when the particle spacing is equal to 6 nm, the separation pressures between kaolinite, illite and montmorillonite are 0.089R, 0.071R and 0.013R, respectively. Therefore, the separation pressure of the three mineral components increases with the increase of the particle spacing. However, when the particle spacing is constant, the separation pressure of kaolinite and illite is not different; instead, it is about one order of magnitude lower than that of montmorillonite. This is mainly due to the different charge densities on the surface of the minerals. From Equation (22), it can be seen that the influence of the surface force on the separation pressure between particles is proportional to the charge density on the surface of the minerals. This conclusion is confirmed by the existing literature [48].

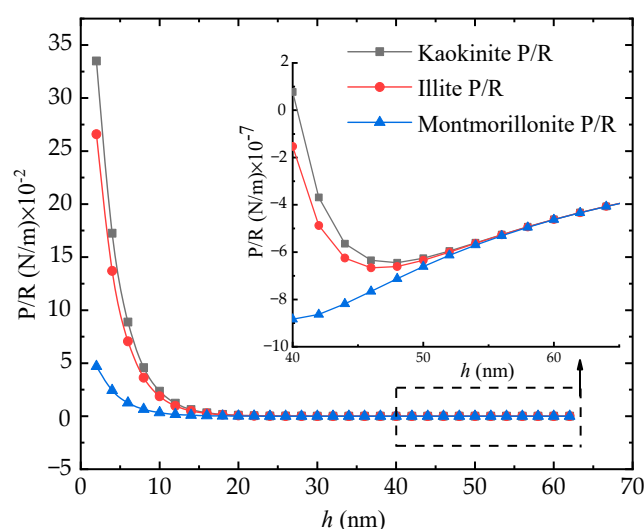


Figure 5. Effect of different minerals of clay on separation pressure between particles.

5.3. Effect of Solution Concentration on Separation Pressure between Adjacent Clay Particles

It can be seen from Table 2 that, although the surface potential of kaolinite is about three times that of montmorillonite, it has no effect on the Debye length k^{-1} . Therefore, it can be considered that the influence of solution concentration on the separation pressure between particles is mainly realized by affecting the Debye constant. Taking the NaCl solution as an example, by substituting the relevant parameters in Table 2 into Equation (22), the effect of different solute concentrations ($0.01 \text{ mol}\cdot\text{m}^{-3}$, $0.1 \text{ mol}\cdot\text{m}^{-3}$, $1 \text{ mol}\cdot\text{m}^{-3}$ and $10 \text{ mol}\cdot\text{m}^{-3}$) on the separation pressure between adjacent clay particles is calculated, the results are shown in Figure 6.

It can be seen from Figure 6 that, with the increase of solution concentration, the separation pressure between particles caused by surface force decreases significantly and finally tends to move toward a stable value. This phenomenon is consistent with the conclusion obtained in the literature [49]. Taking the adjacent clay particles with a spacing of 2 nm as an example, when the solution concentration is lower than $0.1 \text{ mol}\cdot\text{m}^{-3}$, the solution concentration expands by 10 times, resulting in a separation pressure change rate of only 0.037% between clay particles due to surface forces. However, when the solution concentration is higher than $0.1 \text{ mol}\cdot\text{m}^{-3}$, the solution concentration increases by 10 times, which leads to the change rate of interparticle separation pressure caused by surface force up to 0.37%. It can be seen that when the solution concentration is less than a certain threshold, the effect of the solution content on the separation pressure between particles can be ignored.

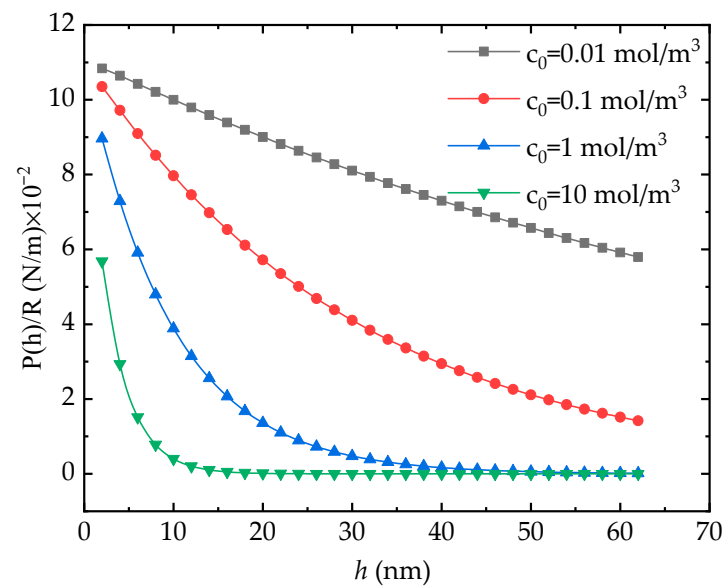


Figure 6. Effect of different solution concentration on separation pressure between adjacent clay particles.

It can be seen from Figure 6 that the variation trend of the inter-particle separation pressure with the increase of the inter-particle distance with the high solution concentration is more stable than that of the low solution concentration with the increase of the inter-particle distance. The main reason is that the higher the concentration of the solution, the smaller the k^{-1} value; that is, the thickness of the diffusion layer formed by the charged particles in the solution is smaller, which makes the thickness of the water film between the particles thinner. As a result, the separation pressure between particles changes rapidly and tends to be stable at first. Therefore, during the freezing process, it can be considered that the higher the solution concentration, the more unfavorable the formation of soil cracks.

6. Conclusions

In this study, the generalized colloidal stability theory was applied to the frost heave process. Through the relationship between the pore throat's radius and the freezing temperature, the separation pressure expression between adjacent frozen clay particles was established and the intrinsic connection between soil cracks and the formation of new ice lenses was revealed. Through our theoretical analysis and verification, the following conclusions can be drawn:

1. We considered the effect of the surface charge of the clay particles and took the ice pressure as the destructive force of the connection between the frozen clay particles; a generalized expression of the separation pressure between the frozen clay particles was obtained through the soil meso-mechanical equilibrium relationship. From the molecular point of view, the effect of the separation pressure between clay particles on the crack development and the formation of new lenses was revealed and verified by experiments.
2. The surface spacing of adjacent charged particles is a single-valued function of their separation pressure, but temperature is the main factor affecting the separation pressure between frozen adjacent clay particles. In the process of soil freezing, the repulsive force caused by the overlap of diffusion double layers is formed on the surface of adjacent charged clay particles in aqueous solution, which makes the microcracks between soil particles take precedence over the formation of a new lens and provides a channel for the migration of water in soil to the ice lens.
3. The effect of surface force on the separation pressure between clay particles is proportional to the surface-charge density of minerals. The separation pressure of different

kinds of minerals shows a similar trend with the increase of spacing, but due to the difference of surface-charge density, the separation pressure of kaolinite and illite are close to each other at the same space, but their values are about one order of magnitude lower than montmorillonite.

4. The separation pressure between adjacent clay particles is negatively correlated with the solution concentration. When the solution concentration is less than $0.1 \text{ mol}\cdot\text{m}^{-3}$, the effect of the solution content on the separation pressure between particles can be ignored. During the freezing process, the higher the solution concentration, the less conducive it is to the development of soil cracks.

Author Contributions: Conceptualization, X.L. and H.C. (Hanqing Chen); methodology, X.L. and H.C. (Hua Cheng); validation, X.L., L.G. and Y.F.; formal analysis, X.L. and X.W.; investigation, X.L. and Y.F.; resources, L.G.; data curation, X.L. and H.C. (Hua Cheng); writing—original draft preparation, X.L.; writing—review and editing, H.C. (Hua Cheng) and H.C. (Hanqing Chen); project administration, L.G.; funding acquisition, X.L. and H.C. (Hua Cheng). All authors have read and agreed to the published version of the manuscript.

Funding: This research was funded by the National Natural Science Foundation of China (No.51874005) and the Anhui University Scientific Research Project (YJS20210386).

Data Availability Statement: Note applicable.

Acknowledgments: The authors extend their appreciation to the National Natural Science Foundation of China (No. 51874005) and the Researchers Supporting Project number (YJS20210386).

Conflicts of Interest: The authors declare no conflict of interest.

References

1. Xu, X.Z.; Wang, J.C.; Zhang, L.X. *Physics of Frozen Soil*, 2nd ed.; Science Press: Beijing, China, 2010; pp. 41–42, ISBN 9787030288677.
2. Jin, H.J.; Yu, W.B.; Gao, X.F.; Cheng, Y.C.; Yao, Z.X. Stability of engineering foundations of oil pipelines in permafrost regions. *Oil Gas Sto. Trans.* **2006**, *25*, 13–18.
3. Wang, J.C.; Wu, Q.B. Settlement analysis of embankment bridge transition section in the permafrost regions of Qinghai-Tibet Railway. *J. Glaciol. Geocryol.* **2017**, *39*, 79–85.
4. Akagawa, S. Experimental study of frozen fringe characteristics. *Cold. Reg. Sci. Technol.* **1988**, *15*, 209–223. [[CrossRef](#)]
5. Konrad, J.M. A mechanistic theory of ice lens formation in fine-grained soils. *Can. Geotech. J.* **1980**, *17*, 473–486. [[CrossRef](#)]
6. Ji, Y.K.; Zhou, G.Q.; Zhou, Y.; Vandeginste, V. Frost heave in freezing soils: A quasi-static model for ice lens growth. *Cold. Reg. Sci. Technol.* **2019**, *158*, 10–17. [[CrossRef](#)]
7. Talamucci, F. Freezing processes in porous media: Formation of ice lenses, swelling of the soil. *Math. Comput. Model.* **2003**, *37*, 595–602. [[CrossRef](#)]
8. Römken, M.; Miller, R.D. Migration of mineral particles in ice with a temperature gradient. *J. Colloid Interf. Sci.* **1973**, *42*, 103–111. [[CrossRef](#)]
9. Peppin, S.; Style, R.W. The Physics of Frost Heave and Ice-Lens Growth. *Vadose Zone J.* **2013**, *12*, 1–12. [[CrossRef](#)]
10. Xia, D.D. Frost Heave Studies Using Digital Photographic Technique. Master's Thesis, University of Alberta, Edmonton, AB, Canada, 2006; pp. 165–169.
11. Arenson, L.U.; Segó, D.C. A New Hypothesis on Ice Lens Formation in Frost-Susceptible Soils. In Proceedings of the 9th International Conference on Permafrost, University of Alaska, Fairbanks, AK, USA, 29 June–3 July 2008; pp. 59–64.
12. Konrad, J.M.; Duquenois, C. A model for water transport and ice lensing in freezing soils. *Water. Resour. Res.* **1993**, *29*, 3109–3124. [[CrossRef](#)]
13. Azmatch, T.F.; Segó, D.C.; Arenson, L.U.; Biggar, K.W. New ice lens initiation condition for frost heave in fine-grained soils. *Cold. Reg. Sci. Technol.* **2012**, *82*, 8–13. [[CrossRef](#)]
14. Zhou, G.Q.; Zhou, Y.; Hu, K.; Wang, Y.J.; Shang, X.Y. Separate-ice frost heave model for one-dimensional soil freezing process. *Acta Geotech.* **2018**, *13*, 207–217. [[CrossRef](#)]
15. Azmatch, T.F.; Arenson, L.U.; Segó, D.C.; Biggar, K.W. Measuring Ice Lens Growth and Development of Soil Strains during Frost Penetration Using Particle Image Velocimetry (Geo PIV). In Proceedings of the 9th International Conference on Permafrost, University of Alaska, Fairbanks, AK, USA, 29 June–3 July 2008.
16. Style, R.W.; Peppin, S.; Cocks, A.; Wettlaufer, J.S. Ice-lens formation and geometrical supercooling in soils and other colloidal materials. *Phy. Rev. E* **2011**, *84*, 041402. [[CrossRef](#)] [[PubMed](#)]
17. Miller, R. Frost heaving in non-colloidal soils. In Proceedings of the 3rd International Permafrost Conference, Edmonton, AB, Canada, 10–13 July 1978; pp. 707–713.
18. Harlan, R.L. Analysis of coupled heat-fluid transport in partially frozen soil. *Water Resour. Res.* **1973**, *9*, 1314–1323. [[CrossRef](#)]

19. Nixon, J.F. Discrete ice lens theory for frost heave beneath pipelines. *Can. Geotech. J.* **1992**, *29*, 487–497. [[CrossRef](#)]
20. Zhou, Y.; Zhou, G.Q. Intermittent freezing mode to reduce frost heave in freezing soils—Experiments and mechanism analysis. *Can. Geotech. J.* **2012**, *49*, 686–693. [[CrossRef](#)]
21. Zeng, G.J.; Zhang, M.Y.; Li, Z.P.; Yuan, H.Y. Analysis and Discussion on mechanical criterion of ice lens formation in frozen soil. *J. Glaciol. Geocryol.* **2015**, *37*, 192–201. [[CrossRef](#)]
22. Derjaguin, B.V.; Churaev, N.V. Structural component of disjoining pressure. *J. Colloid Interf. Sci.* **1974**, *49*, 249–255. [[CrossRef](#)]
23. Gonçalves, J.; Rousseau-Gueutin, P.; De Marsily, G.; Cosenza, P.; Violette, S. What is the significance of pore pressure in a saturated shale layer? *Water Resour. Res.* **2010**, *46*, W04514. [[CrossRef](#)]
24. Style, R.W.; Peppin, S.S.L. The kinetics of ice-lens growth in porous media. *J. Fluid. Mech.* **2012**, *692*, 482–498. [[CrossRef](#)]
25. Rempel, A.W.; Wettlaufer, J.S.; Worster, M.G. Interfacial Premelting and the Thermomolecular Force. *Phys. Rev. Lett.* **2001**, *87*, 088501. [[CrossRef](#)]
26. Rempel, A.W. Formation of ice lenses and frost heave. *J. Geophys. Res. Earth Surf.* **2007**, *112*, F02S21. [[CrossRef](#)]
27. Rempel, A.W.; Wettlaufer, J.S.; Worster, M.G. Premelting dynamics in a continuum model of frost heave. *J. Fluid. Mech.* **2004**, *498*, 227–244. [[CrossRef](#)]
28. Israelachvili, J.N. *Intermolecular and Surface Forces*, 3rd ed.; Academic Press: New York, NY, USA, 2010; pp. 190–195.
29. Hu, F.N.; Xu, C.Y.; Li, H.; Li, S.; Yu, Z.H.; Li, Y.; He, X.H. Particles interaction forces and their effects on soil aggregates breakdown. *Soil. Till. Res.* **2015**, *147*, 1–9. [[CrossRef](#)]
30. Churaev, N.V.; Sobolev, V.D. Disjoining Pressure of Thin Unfreezing Water Layers between the Pore Walls and Ice in Porous Bodies. *Colloid J.* **2002**, *64*, 508–511. [[CrossRef](#)]
31. Zhao, Y.F. *Physical Mechanics of Surfaces and Interfaces*; Science Press: Beijing, China, 2012; pp. 41–52, ISBN 9787030357861.
32. Derjaguin, V.B. Untersuchungen über die reibung und adhesion. *Kolloid-Z.* **1934**, *69*, 155–164. [[CrossRef](#)]
33. Chen, H.; Chen, H.Q.; Cao, G.Y.; Rong, C.X.; Yao, Z.S.; Cai, H.B. Frozen soil capillary-film moisture transport mechanism and its experimental verification. *Chin. J. Geotech. Eng.* **2020**, *42*, 1790–1799. [[CrossRef](#)]
34. Dash, J.G.; Fu, H.; Wettlaufer, J.S. The premelting of ice and its environmental consequences. *Rep. Prog. Phys.* **1995**, *58*, 115–167. [[CrossRef](#)]
35. Peppin, S.S.L.; Elliott, J.A.W.; Worster, M.G. Solidification of colloidal suspensions. *J. Fluid. Mech.* **2006**, *554*, 147–166. [[CrossRef](#)]
36. Gilpin, R.R. A model for the prediction of ice lensing and frost heave in soils. *Water. Resour. Res.* **1980**, *16*, 918–930. [[CrossRef](#)]
37. Wood, P.J.; Williams, J.A. Internal stresses in frozen ground. *Can. Geotech. J.* **1986**, *23*, 409–410. [[CrossRef](#)]
38. Watanabe, K.; Wake, T. Measurement of unfrozen water content and relative permittivity of frozen unsaturated soil using NMR and TDR. *Cold. Reg. Sci. Technol.* **2009**, *59*, 34–41. [[CrossRef](#)]
39. Mackay, J.R. The origin of hummocks, western Arctic coast, Canada. *Can. J. Earth Sci.* **1980**, *17*, 996–1006. [[CrossRef](#)]
40. Chen, L.; Yu, W.B.; Lu, Y.; Wu, P.; Han, F.L. Characteristics of heat fluxes of an oil pipeline armed with thermosyphons in permafrost regions. *Appl. Therm. Eng.* **2021**, *190*, 116694. [[CrossRef](#)]
41. Chen, L.; Voss, C.; Fortier, D.; McKenzie, J. Surface energy balance of sub-Arctic roads with varying snow regimes and properties in permafrost regions. *Permafr. Periglac. Processes* **2021**, *32*, 681–701. [[CrossRef](#)]
42. Gee, G.W.; Bauder, J.W.A. Methods of Soil Analysis. *Soil Sci. Soc. Am. J.* **1986**, *146*, 413–423. [[CrossRef](#)]
43. Shang, J.Q.; Lo, K.Y.; Quigley, R.M. Quantitative determination of potential distribution in Stern-Gouy double-layer model. *Can. Geotech. J.* **1994**, *31*, 624–636. [[CrossRef](#)]
44. Jin, X.; Yang, W.; Meng, X.H.; Lei, L.L. Theoretical deduction and application of unfrozen water content in frozen soil based on electric double layer model. *Chin. J. Rock Mech. Eng.* **2019**, *40*, 1449–1456. [[CrossRef](#)]
45. Yao, Z.S.; Fang, Y.; Zhang, P.; Huang, X.W. Experimental Study on Durability of Hybrid Fiber-Reinforced Concrete in Deep Alluvium Frozen Shaft Lining. *Crystals* **2021**, *11*, 725. [[CrossRef](#)]
46. Fang, Y.; Yao, Z.S.; Hang, X.W.; Li, X.W.; Diao, N.H.; Hu, K.; Li, H. Permeability evolution characteristics and microanalysis of reactive power concrete of drilling shaft lining under stress-seepage coupling. *Constr. Build. Mater.* **2022**, *331*, 127336. [[CrossRef](#)]
47. Watanabe, K.; Flury, M. Capillary bundle model of hydraulic conductivity for frozen soil. *Water. Resour. Res.* **2008**, *44*, W12402. [[CrossRef](#)]
48. Quirk, J.P.; Pereira, C.; Tanton, T.W. Soil Permeability in Relation to Sodicity and Salinity [and Discussion]. *Philos. Trans. R. Soc. Lond. Ser. A* **1986**, *316*, 297–317. [[CrossRef](#)]
49. Mcguiggan, P.M.; Pashley, R.M. Molecular Layering in Thin Aqueous Films. *J. Phys. Chem.* **1988**, *92*, 1235–1239. [[CrossRef](#)]